

Spin Filtered Edge States and Quantum Hall Effect in Graphene

Dmitry A. Abanin, Patrick A. Lee, Leonid S. Levitov

Department of Physics, Massachusetts Institute of Technology, 77 Massachusetts Ave, Cambridge, MA 02139

Electron edge states in graphene in the Quantum Hall effect regime can carry both charge and spin. We show that spin splitting of the zeroth Landau level gives rise to counterpropagating modes with opposite spin polarization. These chiral spin modes lead to a rich variety of spin current states, depending on the spin flip rate. A method to control the latter locally is proposed. We estimate Zeeman spin splitting enhanced by exchange, and obtain a spin gap of a few hundred Kelvin.

A new electron system with low carrier density and high mobility was recently realized in two-dimensional graphene [1]. By varying the carrier density with a gate one can explore a range of interesting states, in particular the anomalous quantum Hall effect [2, 3] (QHE). In contrast to the well-known integer QHE in silicon MOSFETs [4] the QHE in graphene occurs at half-integer multiples of 4, the degeneracy due to spin and orbit. This has been called the half-integer QHE. The unusually large Landau level spacing makes QHE in graphene observable at temperatures of 100 K and higher.

Here we explore the spin effects in graphene QHE. In the presence of Zeeman splitting transport in graphene is described by an unusual set of edge states which we shall call chiral spin edge states. These states are reminiscent of the ordinary QHE edge states [5], but can propagate in opposite directions for opposite spin polarizations. (As shown in [6], similar states can arise due to spin-orbit coupling in the absence of magnetic field. However, the weakness of spin-orbital effects makes the corresponding spin gap quite small.) The chiral spin edge modes can be used to realize an interesting spin transport regime, in which spin and charge currents can be controlled independently. Observation of these phenomena is facilitated by fairly large magnitude of the spin gap. The gap is enhanced due to electron correlation and exchange, and can reach a few hundred Kelvin for realistic magnetic field.

The half-integer QHE in graphene was interpreted in terms of a quantum anomaly of the zeroth Landau level [7]. Alternatively, these properties are easily understood from the edge states viewpoint, similar to the usual QHE. This was done in Ref. [8] using numerical treatment of the zigzag edge. Here we present a continuum description of the edge states, using the massless Dirac model [9] which provides a good approximation for Carbon π -electron band near its center. We reduce the problem to a one-dimensional Schrödinger equation with a potential which depends on the boundary type. By comparing the behavior for armchair and zigzag boundary, we show that the energy spectrum properties near the edge are universal and imply the half-integer QHE.

To interpret the half-integer QHE, let us inspect the energies of the first few Landau levels (LL) obtained for an armchair boundary (Fig. 1(a)). First we ignore electron spin. In the bulk the LL's are doubly degenerate,

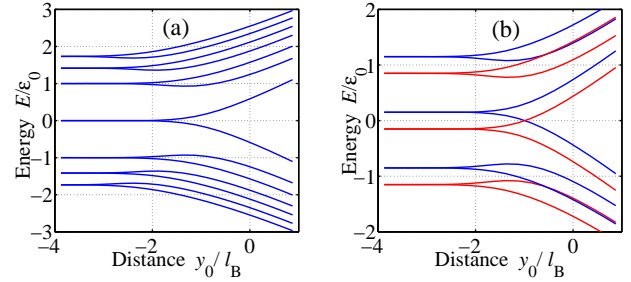


FIG. 1: (a) Graphene energy spectrum near the armchair boundary obtained from Dirac model, Eq.(1). The boundary condition, Eq.(5), lifts the K, K' degeneracy. The odd integer numbers of edge modes lead to the half-integer QHE. (b) Spin-split graphene edge states: the blue (red) curves represent the spin up (spin down) states. These states propagate in opposite directions at zero energy.

due to two species of Dirac particles located near K and K' , the inequivalent corners of the first Brillouin zone. We note that the zeroth LL splits into two levels with positive and negative energies. In contrast, the behavior of the edge states associated with higher LL's is more conventional [5]: the energies of positive (negative) LL's increase (decrease) as one approaches the boundary. Hence in the spinless case the number of edge states can take only odd integer values and the Hall conductivity is odd integer in units of e^2/h . For example, when the chemical potential is between the $n = -1$ and $n = -2$ LL's, there are three branches of active edge states: two of them derived from the LL with $n = -1$ and one from the LL with $n = 0$. As a result, although each Landau level filling factor is an integer, the conductance at QHE plateaus is half-integer in units of $4e^2/h$ which accounts for both the K, K' and spin degeneracy.

This behavior is modified in an interesting way by the spin splitting of LL's (Fig. 1(b)). When the chemical potential μ lies in the interval $-\frac{1}{2}\Delta_s < \mu < \frac{1}{2}\Delta_s$, the zeroth LL is spin polarized, with only spin down states being filled. However, there exists a branch of up-spin edge states going to negative energies. The states of this branch with $\varepsilon < \mu$ will be filled and will contribute to transport on equal footing with the down-spin states. Notably, the up-spin and down-spin states have opposite chiralities, i.e. they propagate in opposite directions. These states carry opposite charge currents but equal spin currents. As a result, the edge transport in the spin

gap, $-\frac{1}{2}\Delta_s < \mu < \frac{1}{2}\Delta_s$, can be spin filtered.

The chiral spin edge states found here are similar to those predicted by Kane and Mele [6], who considered spin-orbit coupling in graphene in the absence of Zeeman field. They obtain a spin gap which is solely due to the spin-orbit coupling and is estimated as $\Delta_{SO} \sim 1$ K [6]. The small gap poses strong constraints on the amount of disorder and on temperature, hindering experimental tests of the interesting predictions of Ref. [6]. In contrast, the magnetic field-induced gap is quite large: the Zeeman energy of $\Delta_s = g\mu_B B \sim 15$ K at $B \sim 10$ T is further enhanced by exchange interaction, putting it in an experimentally convenient range of hundreds of Kelvin. Furthermore, one can alter the character of spin flip scattering at the edge to induce backscattering among the spin polarized edge modes, enabling experimental observation of a number of novel transport effects (see below).

To analyze the edge states, we employ the Dirac model [9] which describes the low-lying states as linear combinations of four zero-energy Bloch functions with slow varying envelope functions $u_K, v_K, u_{K'}, v_{K'}$. Here u and v correspond to the wave function components on two inequivalent atomic sites A, B , and the subscripts K, K' denote the inequivalent Dirac points. The effective low-energy Hamiltonian, written near each of the points K, K' in terms of $u_{K,K'}, v_{K,K'}$, is of the form

$$H_K = v_0 \begin{bmatrix} 0 & \tilde{p}_+ \\ \tilde{p}_- & 0 \end{bmatrix}, \quad H_{K'} = v_0 \begin{bmatrix} 0 & \tilde{p}_- \\ \tilde{p}_+ & 0 \end{bmatrix}, \quad (1)$$

where $\tilde{p}_\pm = \tilde{p}_x \pm i\tilde{p}_y$, $\tilde{p}_\mu = p_\mu - \frac{e}{c}A_\mu$ and $v_0 \approx 8 \times 10^7$ cm/s is Fermi velocity. The energy spectrum in the bulk is

$$E_n = \text{sgn}(n)|n|^{1/2}\varepsilon_0, \quad \varepsilon_0 = \hbar v_0 (2eB/\hbar c)^{1/2} \quad (2)$$

with integer n . For typical magnetic field of 10 T, the lowest LL separation is estimated to be quite large, $\varepsilon_0 = E_1 - E_0 \approx 1000$ K. We now consider a graphene sample with an armchair edge parallel to the x axis, using Landau gauge $A_x = -By$, $A_y = 0$. We eliminate the v components of the wave function and consider the eigenvalue equations for the u components:

$$\frac{1}{2} (p_y^2 + (y - y_0)^2 + 1) u_K = (E/\varepsilon_0)^2 u_K, \quad (3)$$

$$\frac{1}{2} (p_y^2 + (y - y_0)^2 - 1) u_{K'} = (E/\varepsilon_0)^2 u_{K'}, \quad (4)$$

where $y_0 = -p_x$. Here x, y and p_x, p_y are measured in the units of $\ell_B = (\hbar c/eB)^{1/2}$ and \hbar/ℓ_B .

To obtain the energy spectrum near the edge, one needs to supplement Eqs.(3),(4) with suitable boundary conditions. We obtain the latter from the tight-binding model assuming that it is valid up to the very last row near the boundary. In the armchair case the boundary condition requires the wave function to vanish at both A and B lattice sites along the line $y = 0$. For the envelope

functions u, v , taken at $y = 0$, this means

$$u_K = u_{K'}, \quad v_K = v_{K'} \quad (5)$$

(see Ref. [10] for a more general analysis).

Instead of the problem in a halfplane with boundary conditions (5), it is more convenient to consider Eq.(3) on the negative half-axis $y < 0$, and Eq.(4) on the positive half-axis $y > 0$. Then the first boundary condition in Eq.(5) implies continuity of the wavefunction at $y = 0$, while the second condition implies continuity of the derivative $\partial u/\partial y$. Therefore the problem reduces to calculating energy levels in the potential

$$V(y) = \frac{1}{2}(|y| - y_0)^2 - \frac{1}{2}\text{sgn}(y), \quad (6)$$

defined on the entire line. Numerical solution of this problem gives the energy dispersion shown in Fig. 1.

We now briefly discuss the zigzag edge, another very common graphene edge type. In the absence of magnetic field this boundary supports a band of low-energy surface states [11, 12]. Wavefunctions of these states decay away from the boundary on a length scale of the order of lattice spacing, which is typically much shorter than the magnetic length ℓ_B . Therefore, the surface states should not be sensitive to the magnetic field. This conclusion is supported by the numerical study [8].

In contrast to the surface states, special for zigzag edge, the LL behavior near the edge is universal and depends on the boundary type only weakly. In the Dirac equation framework, the boundary condition for a zigzag edge is that either A or B components of the envelope function vanish at the boundary, depending on the orientation of the edge. This yields two possible boundary conditions: either $u_K = u_{K'} = 0$ or $v_K = v_{K'} = 0$ at the edge. Finding energy spectrum in this case requires solving Landau level problem with a hard-wall boundary condition, familiar from the usual QHE [5]. The energy spectrum for the zigzag edge, given by the square root of the dispersion curves found in Ref. [5], is qualitatively similar to the one in Fig. 1. These results are consistent with the numerical analysis of Ref. [8].

Turning to the analysis of the spin gap, let us consider the exchange energy for half-filled spin-degenerate Landau level. In the Hartree-Fock approximation, it is given by spin-dependent correlation energy:

$$E = \sum_{i,j=+,-} \frac{1}{2} \int \int V(r - r') g_{ij}(r - r') d^2r d^2r' \quad (7)$$

with $g_{ij}(r - r') = \langle n_i(r) n_j(r') \rangle$ the pair correlation functions. We consider Coulomb interaction of the form $V(\mathbf{r}) = e^2/\kappa r$ with the dielectric constant [14] describing screening due to the filled states, $\varepsilon < 0$.

To describe correlations, we use the result for fully filled Landau level [17], $g_0(r) = 1 - e^{-r^2/2\ell_B^2}$, setting [18]

$$g_{++}(r) = n_+^2 n_0^2 g_0(r), \quad g_{--}(r) = n_-^2 n_0^2 g_0(r), \quad n_0 = \frac{eB}{\hbar c},$$

where n_{\pm} are the occupation fractions of the up and down spin states, $n_{+} + n_{-} = 1$. We model the Coulomb interaction-induced correlations of particles with opposite spin, which are absent for noninteracting electrons, by $g_{+-} = n_{+}n_{-}n_0^2(1 - \alpha e^{-r^2/2\ell_B^2})$, where $\alpha < 1$ describes relative strength of Coulomb and exchange correlations. This approach yields

$$E_{\text{exchange}} = -An_{+}n_{-}, \quad A = \left(\frac{\pi}{2}\right)^{1/2} \frac{e^2}{\kappa\ell_B}(1 - \alpha). \quad (8)$$

To estimate spin polarization, we consider Gibbs free energy per particle for the half-filled spin degenerate Landau level, $G/N = E - TS$, where

$$S = -T \sum_{i=\pm} n_i \ln n_i, \quad E = \frac{1}{2}E_Z(n_{+} - n_{-}) - An_{+}n_{-},$$

with E_Z the Zeeman energy. The ground state, determined by $\delta G = 0$ with $n_{+} + n_{-} = 1$, satisfies

$$T \ln(n_{+}/n_{-}) - E_Z + A(n_{-} - n_{+}) = 0. \quad (9)$$

In the absence of exchange interaction, $A = 0$, this would give $n_{-}/n_{+} = e^{-E_Z/T}$. The more realistic case of exchange A large compared to E_Z can be analyzed by setting $E_Z = 0$. In this case we have a phase transition at $T_c = \frac{1}{2}A$. At low temperature, $T \ll T_c$, the concentrations n_{\pm} satisfy $n_{-}/n_{+} = e^{-A/T}$, i.e. the spin gap at $T \ll T_c$ can be estimated as $\Delta = A$.

To obtain numerical value of Δ , we use the RPA estimate of the screening function [14], with $e^2/hv \approx 2.7$:

$$\kappa = 1 + 2\pi e^2 \cdot \frac{1}{4\hbar v} \approx 5.24. \quad (10)$$

Comparing to the LL separation ε_0 , Eq.(2),

$$\Delta = \frac{\pi^{1/2}e^2}{2\kappa\hbar v}(1 - \alpha)\varepsilon_0 \approx 0.456 \cdot (1 - \alpha)\varepsilon_0. \quad (11)$$

Note that Δ is proportional to the Dirac LL energy ε_0 and scales as $B^{1/2}$, in contrast to the Zeeman energy. If we use $\alpha = 0$, i.e. ignore correlations of electrons with opposite spins, we obtain $\Delta \simeq 450$ K for $B \simeq 10$ T. (This approximation, while giving correct order of magnitude, may somewhat overestimate the exchange contribution.)

We now discuss possible experimental tests of the chiral spin edge states, using the four-terminal device shown in Figs. 2,3. We assume that each contact injects both spin polarizations with the same voltage V_k , i.e. full spin mixing takes place in the leads. The *charge* current flowing out of the k -th contact is given by

$$I_k^c = \sum_{k'} g_{kk'} (V_k - V_{k'}), \quad (12)$$

where $g_{kk'}$ is the Landauer conductance of the edge channel connecting contacts k and k' , and V_k are voltages on

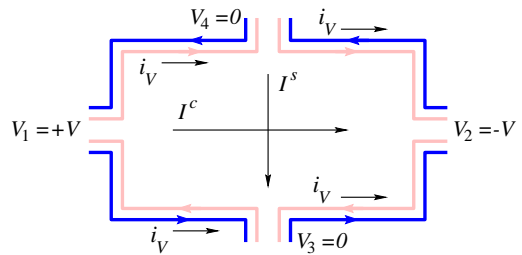


FIG. 2: Four-terminal device with chiral spin edge states (no backscattering). In response to charge current of $I^c = 2i_V = 4e^2V/h$ between reservoirs 1 and 2, pure spin current of $I^s = 2i_V$ flows between 4 and 3, while Hall voltage is zero.

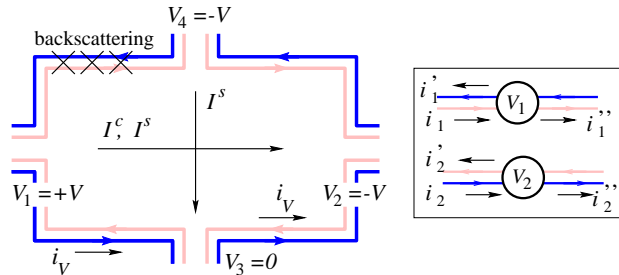


FIG. 3: Same as in Fig. 2 with backscattering between edge states induced by altering local spin-flip rate. Strong backscattering gives rise to asymmetric current flow with the current between 1 and 2 fully spin polarized. Inset shows how Hall voltage probe can be used to detect spin current.

the contacts. In the presence of backscattering among the edge states, the conductance $g_{kk'}$ can be expressed in terms of transmission matrix $T_{kk'}$ of the edge channels [13], with $g_{kk'} = T_{kk'}e^2/h$. The voltage probes are defined by the condition $I_k^c = 0$ and Eq.(12) is solved for the current and voltage at each contact [13].

The *spin current* is then determined as follows. The spin current flowing from the reservoir k to reservoir k' is given by the sum of outgoing current of e^2V_k/h , reflected current $(1 - T_{kk'})e^2V_k/h$ and the current from k' -th reservoir, $T_{kk'}e^2V_{k'}/h$. We obtain $I_{kk'}^s = \pm [(2 - T_{kk'})V_k + T_{kk'}V_{k'}]e^2/h$ (the three contributions to the spin current are of the same sign, plus if the channel $k \rightarrow k'$ is spin up and minus if it is spin down). Thus the total spin current flowing out of the k -th contact is

$$I_k^s = \sum_{k'} I_{kk'}^s = \sum_{k'} \varepsilon_{kk'} g_{kk'} (V_k - V_{k'}), \quad (13)$$

where $\varepsilon_{kk'} = -\varepsilon_{k'k}$ equals +1 (-1) when the current from k to k' is carried by spin up (spin down) electrons.

The general relations (12), (13) become more transparent in two simple limiting cases, illustrated in Figs. 2, 3. First we inspect the clean limit with no backscattering at the edge (Fig. 2). Applying voltage of $2V$ between contacts 1 and 2 we obtain pure *spin current* across the sample equal to $2i_V$, where $i_V = e^2V/h$. There is also charge current of $2i_V$ between 1 and 2 and no Hall voltage, yielding $\rho_{xx} = h/2e^2$.

Alternatively, let us introduce strong backscattering in

the shoulder connecting 1 and 4, such that the resistance between 1 and 4 is infinite, while all the other shoulders are clean (Fig. 3). Such a system acts as a “spin filter”. Indeed, the current flowing from 1 to 2 is *spin polarized*. The Hall voltage in this case is nonzero, equal to the half of the voltage between 1 and 2.

Interestingly, the Hall voltage measures spin current rather than charge current. This is illustrated by Fig. 3 inset which depicts currents i_1, i_2 that flow into the voltage probes, equilibrate and flow out ($i'_{1,2} = \frac{1}{2}i_{1,2}$). The Hall voltage is proportional to the incoming *spin* current:

$$V_1 - V_2 = \frac{1}{2}(i_1 - i_2)h/e^2 = -I_s \cdot h/2e^2. \quad (14)$$

Such voltage probes can be attached to the top or bottom leads in Fig. 2, 3 to verify the presence of spin currents. (We caution that currents i_1, i_2 are affected by the probes and should be calculated self-consistently using (12).)

We now discuss spin-flip scattering mechanisms. One can make qualitative observations which (a) show that spin-flip scattering is strongly suppressed and (b) suggest a way to manipulate it. We assume that the main source of the spin-flip scattering is spin-orbit (SO) interaction, which includes the intrinsic term proportional to σ_z and the Rashba term [6]. The former interaction is ineffective when electron spins are polarized along the z axis, amounting merely to an energy shift of the order of $\Delta_{SO} \sim 1$ K, without the up-down spin mixing. At the same time, the Rashba term turns out to be extremely small, $\lambda_R \sim 0.5$ mK [6], making spin-flips negligible.

The situation changes, however, when an *in-plane magnetic field* is applied. Now the intrinsic SO interaction admixes the spin projections along the tilted field, leading to a small avoided crossing of the chiral spin edge states of magnitude Δ_{SO} . Using a local gate one can detune from this crossing by $\Delta E \gg \Delta_{SO}$. In this case, the spin-flip scattering probability is estimated as $\Delta_{SO}^2/\Delta E^2$, which gives a factor of 10^{-2} for $\Delta E \sim 10$ K. The spin-flip scattering rate will be further reduced if the disorder at the edge has a short length scale compared to ℓ_B (recent STM experiments [15, 16] report $a \sim 1$ nm). For typical magnetic length, $\ell_B \sim 10$ nm at $B \sim 10$ T, this gives spin-flip scattering suppressed by a factor of $a^2/\ell_B^2 \sim 10^{-2}$. These observations show that backscattering at the edge should be strongly suppressed and suggest that by gating the QHE edge in the presence of in-plane magnetic field one can control local spin-flip rates independently. In particular, by tuning ΔE to zero in one shoulder of the four terminal device, one could realize the situation depicted in Fig. 3.

Up to now we have focused on the LL spin splitting and ignored the orbital K, K' degeneracy. However, the exchange effects must lift the K, K' degeneracy as well. Moreover, the K, K' exchange gap should be of the same size as the spin gap Δ since electron interaction has the same strength for different spin and valley species ($SU(4)$

symmetry). The spontaneously appearing order parameter will have orientation fixed by weak nonsymmetric interactions, the difference between the intra and inter-sublattice coupling for K, K' , and the Zeeman energy for spin splitting. The spin filter effects discussed above assume that spin splitting occurs before orbital splitting.

We conclude by addressing the experimental situation. Our theory predicts a plateau of $R_{xy} = 0$ between $eV = \pm \frac{1}{2}\Delta$ which was observed in a recent experiment [19]. This paper also reports full lifting of the four-fold degeneracy of the zeroth LL at high magnetic fields $B > 10$ T which is consistent with the predicted strength of K, K' exchange. We attribute the suppression of the zeroth LL splitting at lower magnetic fields to the disorder present in the currently available samples [20]. The observed value of R_{xx} at $B = 25$ T is about 40 k Ω . According to our picture, this means that the chiral edge states are not localized and transmission coefficients of the edge channels are about 1/3. Thus a spin Hall current may already be present in this case.

After the completion of this work, we became aware of Ref. [21] where a continuum description of the edge states given in the first part of this paper is also reported.

We acknowledge support by NSF grant number DMR-0517222 (PAL) and NSF-NIRT DMR-0304019 (LL).

-
- [1] K. S. Novoselov, *et al.* cond-mat/0410631, Science, **306**, 666 (2004).
 - [2] K. S. Novoselov, *et al.* Nature **438**, 197 (2005).
 - [3] Y. Zhang, *et al.* Nature **438**, 201 (2005).
 - [4] K. v. Klitzing, G. Dorda and M. Pepper, Phys. Rev. Lett. **45**, 494 (1980).
 - [5] B. I. Halperin, Phys. Rev. B **25**, 2185 (1982).
 - [6] C. L. Kane and E. J. Mele, Phys. Rev. Lett. **95**, 226801 (2005).
 - [7] V. P. Gusynin and S. G. Sharapov, Phys. Rev. Lett. **95**, 146801 (2005).
 - [8] N. M. R. Peres, F. Guinea, A. H. Castro Neto, cond-mat/0506709, unpublished.
 - [9] D. P. DiVincenzo and E. J. Mele, Phys. Rev. B **29**, 1685 (1984).
 - [10] E. McCann and V. I. Fal'ko, J. Phys.: Condens. Matter **16**, 2371 (2004).
 - [11] M. Fujita, *et al.* J. Phys. Soc. Jpn. **65**, 1920 (1996).
 - [12] S. Ryu and Y. Hatsugai, Phys. Rev. Lett. **89**, 077002 (2002).
 - [13] M. Büttiker, Phys. Rev. B **38**, 9375 (1988).
 - [14] J. González, F. Guinea, and M. A. H. Vozmediano, Phys. Rev. B **63**, 134421 (2001).
 - [15] Y. Kobayashi, *et al.*, Phys. Rev. B **71**, 193406 (2005).
 - [16] Y. Niimi, *et al.*, cond-mat/0601141, unpublished.
 - [17] B. Jancovici, Phys. Rev. Lett. **46**, 386 (1981).
 - [18] R. B. Laughlin, Phys. Rev. Lett. **50**, 1395 (1983).
 - [19] Y. Zhang, *et al.*, cond-mat/0602649, unpublished.
 - [20] N. A. Sinitsyn, *et al.*, cond-mat/0602598, unpublished.
 - [21] L. Brey and H. A. Fertig, cond-mat/0602505, unpublished.